Organic & Biomolecular Chemistry

Accepted Manuscript

ROYAL SOCIETY OF CHEMISTRY

www.rsc.org/obc

Organic & Biomolecular Chemistry

RSCPublishing

ARTICLE

Phototriggerable peptidomimetics for the inhibition of Mycobacterium turberculosis ribonucleotide reductase by targeting protein-protein binding

Cite this: DOI: 10.1039/x0xx00000x

Received 00th January 2012,
Accepted 00th January 2012

DOI: 10.1039/x0xx00000x

www.rsc.org/

Christoffer Karlsson,[a] Magnus Blom,[a] Miranda Johansson (neé Varedian),[a] Anna M. Jansson,[c] Enzo Scifo,[c] Anders Karlén,[b] Thavendran Govender,[d] Adolf Gogoll[a*]

[a] Department of Chemistry - BMC, Uppsala University, Box 576, S-751 23 Uppsala, Sweden

[b] Department of Medicinal Chemistry, Organic Pharmaceutical Chemistry, Uppsala University, Box 574, S-751 23 Uppsala, Sweden

[c] Department of Cell and Molecular Biology, Structural Biology, Uppsala University, Box 596, S-751 24 Uppsala, Sweden

[d] Catalysis and Peptide Research Unit, University of KwaZulu Natal, Durban 4000, South Africa

Incorporation of an artificial amino acid **2** with a stilbene chromophore into peptidomimetics with three to nine amino acids yields phototriggerable candidates for inhibition of the binding between the R1 and R2 subunits of the *M. tuberculosis* ribonucleotide reductase (RNR). Interstrand hydrogen bond probability was used as a guideline for predicting conformational preferences of the photoisomers. Binding of these inhibitors has been rationalized by docking studies with the R1 unit. Significant differences in binding of the photoisomers were observed. For the shorter peptidomimetics, stronger binding of the *Z* isomer might indicate hydrophobic interactions between the stilbene chromophore and the binding site.

Introduction

Modulation of molecular functionality *via* reversible photochemical reactions constitutes an attractive opportunity to extend the properties of chemical compounds. For example, a compound lacking physiological activity might be administered to an organism, then activated at a location and time of choice by photoirradiation. Peptides and proteins, given their rich diversity of functionality in a physiological context, are particularly enthralling candidates for this concept.[1] Nature has developed examples such as the photoswitchable green fluorescent (GFP) and related proteins.[2] While the majority of photoswitchable peptides and proteins is based on the azobenzene chromophore,[1,3] we have previously introduced the less frequently utilized stilbene chromophore as a viable alternative.[4] For example, it was possible to photomodulate the activity of an artificial hydrolase by replacing a four amino acid segment of its 42 amino acid sequence by a stilbene derivative.[4c]

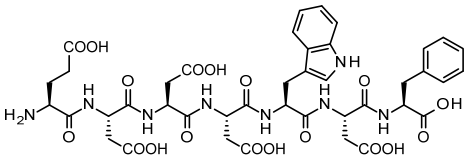

Figure 1: Heptapeptide **1** (Glu-Asp-Asp-Asp-Trp-Asp-Phe) derived from the C-terminal of the R2 subunit of *M. tuberculosis* RNR.

Photoregulation of proteins typically involves incorporation of suitable chromophores into their backbone, or cross-linking of sidechains. In the present study, we investigate another alternative, *i.e.*, to target the assembly of enzyme subdomains. Our target, ribonucleotide reductase (RNR), is an essential enzyme for the synthesis of DNA, catalyzing the reduction of ribonucleotides to their corresponding deoxyribonucleotides.[5] The tetrameric enzyme is composed of two large subunits, R1, and two smaller subunits, R2. The R1 unit contains the binding site for substrates, while the R2 unit is involved in catalysis with its intrinsic tyrosine radical. Catalysis takes place *via* the interplay between the different subunits, by an electron transfer between the radical in R2 and the active site in R1. Inhibition of RNR is relevant not only for the development of new anticancer and antiviral agents, but also for the development of new antitubercular agents.[6] There are several approaches to inhibit RNR, and one of them is to target the interaction between the R1 and R2 subunits. Previous studies have shown that peptide sequences derived from the C-terminal end of the R2 subunit (Figure 1) can compete for the R2 binding site in R1, and thus inhibit the activity of RNR.[7] In particular, the peptide sequence Ac-Glu-Asp-Asp-Asp-Trp-Asp-Phe-OH (Ac-**1**) has shown high potency towards the inhibition of RNR. An interesting observation was that an N-terminal Fmoc-residue appeared to increase the affinity for the R2 binding site.[7a] We thus found it tempting to test whether a photomodulation of this protein-protein interaction might be possible.[8]

Results and Discussion

In an initial attempt to regulate the inhibitory potency of Ac-**1** by external stimulus, we attached stilbene derivative **2** to the N-terminal of this peptide (Scheme 1). By isomerizing the *E* to the

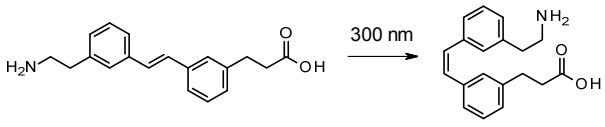

Scheme 1: *Z*-*E* isomerization of the artificial stilbene amino acid **2**.

Z isomer of the stilbene, we expect a change of the conformation of the peptide and thereby a change of affinity to the R2 binding site. Thus, the stilbene chromophore would constitute a phototrigger. In addition, a set of constructs with the phototriggerable unit **2** integrated into more drug-like analogues of Ac-**1**, have been designed and evaluated *in silico*, and subsequently synthesized. These are represented by peptidomimetics **6** – **8** (*vide infra*), which have been subjected to binding studies.

Design of heptapeptide analogues

To test the validity of our initial assumption that the stilbene moiety, structurally similar to Fmoc, might have an impact on the binding properties of peptidic inhibitors for the R1 subunit, a small set of linear peptides **3** – **5** based on the C-terminal heptapeptide of the R2 subunit was synthesized. In these, the artificial amino acid **2** incorporating a *meta* substituted stilbene moiety with a flexible CH_2CH_2-linker was attached to the N-terminal of the heptapeptide (Figure 2).

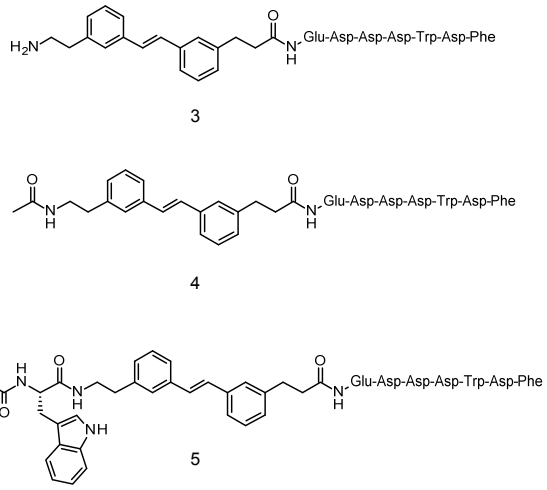

Figure 2: Phototriggerable peptidomimetic analogues of the C-terminal of heptapeptide R2.

Polar interactions are important for the binding of peptidic inhibitors to the R2 binding site.[7a] In compound **3** the charged 2-aminoethyl substituent can be expected to form ionic interactions with any of the six negatively charged carboxylate groups in the peptidomimetic. We anticipated that these ion-ion interactions should be more readily formed in the *Z* isomer as compared to the *E* isomer. If this is true, the *E* isomer should be more potent since the conformation of the heptapeptide should be less perturbed. In peptidomimetic **4** the N-terminal amino group has been acetylated and only H-bonds can be formed instead of the strong ionic interactions, and the difference in activity between the *Z* and *E* isomer should therefore be less

pronounced. Finally in peptidomimetic **5** the bulky N-acetylated Trp amino acid has been attached to the linker

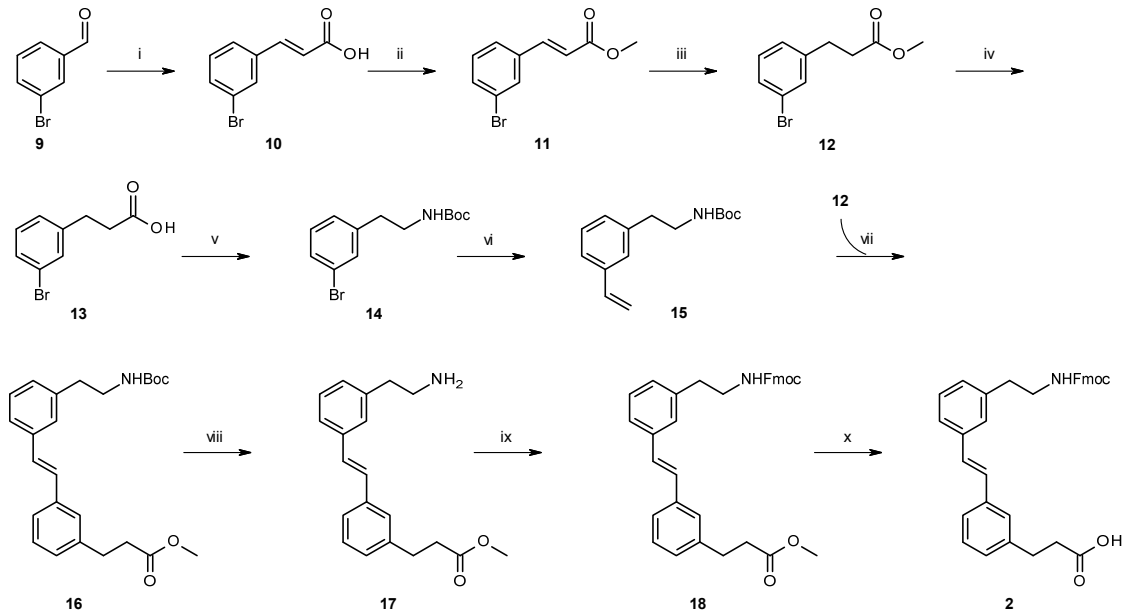

Scheme 2 Synthesis route of the phototriggerable amino acid **2**. i) malonic acid, pyridine, piperidine, 100 °C, 1.5 h, 66 %; ii) MeOH, HCl (conc.), microwave, 130 °C, 50 min, 100 %; iii)$Ni(OAc)_2$, $NaBH_4$, MeOH, EtOAc, H_2 (1 bar), r.t., 2 h, 100 %; iv) NaOH, EtOH, 78 °C, 2 h, 99 % v) NaN_3,Bu_4NBr, $ZnBr_2$, Boc_2O, THF, 40 °C, 48 h, 24 %; vi) $Bu_3SnCH{=}CH_2$, $Pd(PPh_3)_2Cl_2$, LiCl, Et_3N, DMF,microwave, 130 °C, 25 min, 79 %; vii) $Pd(OAc)_2$, $(o\text{-}CH_3C_6H_4)_3P$, Et_3N, DMF, microwave, 120 °C, 30 min, 31 %; viii) TFA (50 % in DCM), 15 min (not isolated); ix) Fmoc-Cl, dioxane, Na_2CO_3 (10 % in H_2O), 24 h (not isolated); x) DCM, HCl (conc.), 120 °C, 17 h, 34 %.

giving a more sterically crowded peptidomimetic in the *Z* conformer as compared to the *E* isomer, which might result in a more pronounced difference between photoisomers.

Synthesis of stilbene amino acid **2**

Compared to our previously reported **s**ynthesis of **2**,[4a] we have modified the scheme to one requiring a single as well as less expensive starting material for both terminals of the stilbene moiety. This avoids the use of 3-bromophenethylamine as starting material. Instead, the substantially less expensive 3-bromobenzaldehyde **9** (approx. 1/50 the cost) is used. The latter is first converted into bromoaryl ester **12** that constitutes the carboxyl terminal of the stilbene derivative. Half of this is converted into a BOC-protected bromoaryl amine **14** using a Curtius rearrangement. The synthesis of BOC-protected amines from carboxylic acids has previously been reported by Lebel and Leogane, using sodium azide and BOC_2O.[9] An alternative, *i.e.*, using DPPA in *t-BuOH* was also tested,[10] but had inferior performance. A further change compared to the previous synthesis was to do the Stille coupling to produce **15** on the BOC-protected amine (**14**), rather than on the unprotected amine. This has some advantages compared to the original synthesis route. Using $Pd(PPh_3)_2Cl_2$, it appeared that the unprotected amine would bind to the catalyst. Also, the protected amine, as opposed to the free amine, can easily be purified by flash chromatography.

Synthesis of peptidomimetics

Preparation of the *E*-isomers of compound **3** – **5** followed standard SPPS protocols.[4b] The corresponding *Z*-isomers were obtained by subsequent photoisomerization through irradiation with UV-light at 300 nm. It should be noted that, according to our observations, the often cited potential dihydrophenanthrene formation during stilbene photoisomerization is not a problem, at least not if only a single isomerization as opposed to several cycles is required.

Binding studies Method A

The analysis is based on displacement of the the N-terminally dansylated RNR-R2 C-terminal heptapeptide Glu-Asp-Asp-Asp-Trp-Asp-Phe.[7i] This probe gave, when bound to R1, a significant fluorescence polarization signal. A quality value Z′ of 0.8 was calculated[11] and is well above the significance limit of 0.5. Displacement of the probe with inhibitor compounds reduces the fluorescence polarization (FP) factor to background level. The degree of polarization was plotted against the log of the inhibitor concentration. For each compound the value for 50% displacement of the fluorescent peptide (DC_{50}) was calculated from the plot and used for ranking of the compounds. Results for peptide Ac-**1** and the three peptidomimetics **3** – **5** are presented in Table 1.

Table 1: Inhibitory potency of phototriggerable heptapeptide derivatives **3** – **5**.

[a] Relative inhibition is presented as DC_{50} **(1)** / DC_{50} (x). [b](DC_{50}(*Z*)-DC_{50}(*E*))/DC_{50}(*E*)·100 %.

Peptide	Inhibition DC_{50} (μM)	Relative inhibition[a]	Inhibition increase upon photosisomerization[b]
Ac-**1**	8	1	
E-**3**	0.35	23	3 %
Z-**3**	0.36	22	
E-**4**	0.11	73	163 %
Z-**4**	0.29	28	
E-**5**	0.09	94	33 %
Z-**5**	0.12	67	

Interestingly, all six peptidomimetics were more potent than Ac-**1**. Whereas the *E* isomer, as expected, was the most potent for **4** and **5**, compound **3** showed no significant difference between the photoisomers. A possible explanation might be the overpowering effect of the ionic interaction as compared to the conformational effect from the rather flexible stilbene moiety. Furthermore, it appears that the stilbene motif itself contributes to the binding interaction, irrespective of its configuration.

Design of shorter analogues

Having established the inhibitory potency of stilbene incorporating peptidomimetics as well as some discrimination between their *Z* and *E* isomers, it was next considered advantageous to devise a peptidomimetic analogue of the known R2 C-terminus with fewer amino acids, since it would be more drug-like as well as more accessible to computational analysis.[12] To design shorter peptides, it was first necessary to determine which residues were most essential for binding to the target R2 binding site. This might be revealed by examining the interaction site between the RNR subunits. By probing the available space in the binding pocket, the optimal position of the stilbene chromophore might also be indicated, with the option to replace some other amino acids.

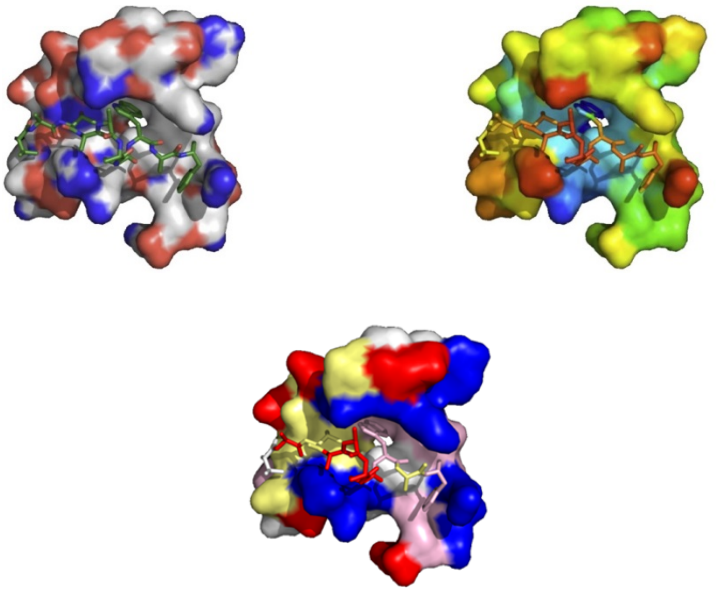

Figure 3: Top left: Positioning of the R2 C-terminal heptapeptide (stick structure) in the R1-R2 interaction site, with atom types indicated by colouring scheme (white/green: carbon, blue: nitrogen, red: oxygen), surface of the R1 subunit shown in white. Top right: Temperature factors (red: least certain position – blue: most certain position) of the R1-R2 interaction site with docked heptapeptide. Bottom: Amino acid residues coloured by type (blue: positive, red: negative, white: hydrophobic, pink: aromatic, yellow polar).

The crystal structure of RNR (2BQ1) has the R2 C-terminal located in a small pocket of the R1 subunit (shown in Figure 3 to the left). Due to its low resolution (not better than 4.0 Å), reliable quantitative data can not be determined. Thus, the structural investigation has to remain qualitative.[13] However, the temperature factors at the interaction site between the subunits (shown in Figure 3 to the right) indicate a somewhat better resolution than for the whole enzyme.[14]

The R1 binding pocket is lined with positively charged residues (Figure 3, bottom), whereas the inside the pocket is more hydrophobic. The R2 C-terminal contains several negative residues (Arg and Glu), which seem to be too distant from the positive residues in R1 for ion bond formation. Regardless, these charges might contribute to the R1-R2 subunit binding, while other residues provide specificity. The most well resolved R2 component in the interaction site, a tryptophan residue, is in

close contact with an aromatic region of R1. Therefore, it constitutes a potentially important residue for specific binding. Indeed, according to a study of an inhibitory heptapeptide (Figure 1) by Nurbo in 2007,[6d] tryptophan and phenylalanine were identified as the most important residues for enzyme inhibition. The removal of either one caused loss of inhibitory effect. Furthermore, subsequent removal of negatively charged heptapeptide residues resulted in gradual decrease of its inhibitory effect. While the function of the C-terminal phenylalanine is uncertain due to poor structural resolution, potential interactions might be inferred from the presence of several aromatic side chains in its vicinity, as well as an arginine that might be involved in a π-cation interaction.

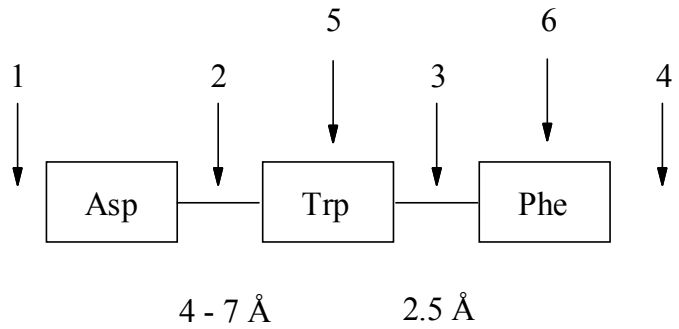

Figure 4: Six conceivable modifications of the inhibitory heptapeptide - introducing the stilbene chromophore on either terminus (1 & 4), between residues (2 & 3), or replacing an aromatic residue with the phototrigger (5 & 6). Asp, Trp and Phe are retained to provide sufficient binding. Distances between the residues in native R2 are indicated.

In summary, phenylalanine and tryptophan appear to be most important for inhibition. Combining these with a few negatively charged residues, *e.g.* aspartate, might increase the inhibitory effect. With these premises, six different types of peptidomimetics, with varying stilbene phototrigger position, were designed (Figure 4): 1) trigger at the N-terminal, 2) trigger between the Asp and Trp residues, 3) trigger between Trp and Phe residues, 4) C-terminal trigger, 5) trigger replacing the Trp, or 6) replacing Phe with the trigger. The possible peptidomimetics in these groups, with at most four amino acids, are shown in Table 2. For practical reasons, peptidomimetics with four residues were at the upper limit of the capability of the conformational search methods used.

In the Trp-Asp-Phe part of the heptapeptide docked to the R2 binding site (Figure 3), the distance between the carbonyl carbon and the α-nitrogen of Asp is 2.5 Å. Since the corresponding distance in the *Z*-stilbene phototrigger is 5.0 Å, inserting the trigger between Trp and Phe (alternative 3) is probably not reasonable. A C-terminal trigger (alternatives 4 and 6) differs considerably from the compounds already tested with inhibitory effect (**3** – **5**), and was therefore considered less interesting. The remaining alternatives 1, 2 and 5 result in peptidomimetics with the trigger being part of a peptidomimetic containing one to four natural amino acids. These peptidomimetics and also two members of group 6 were evaluated computationally by conformational analysis.

Table 2: Peptidomimetics designed according to Figure 4. '+': tested with conformational search. 'x': deemed too large for conformational search.

Group	Peptidomimetic	N-capping	
		Ac	Fmoc
1	Trigger-Asp-Trp-Asp-Phe	+	x
2	Trigger-Trp-Asp-Phe	+	+
	Asp-Trigger-Trp-Asp-Phe	+	x
3	Trp-Trigger-Phe		
	Asp-Trp-Trigger-Phe		
4	Trp-Asp-Phe-Trigger		
	Asp-Trp-Asp-Phe-Trigger		x
5	Trigger-Asp-Phe	+	+
	Asp-Trigger-Asp-Phe	+	
	Trigger-Phe	+	+
	Asp-Trigger-Phe	+	
6	Trp-Asp-Trigger		
	Asp-Trp-Asp-Trigger		
	Trp-Trigger	+	
	Asp-Trp-Trigger	+	

Conformational search

A model compound (Ac-Trigger-Glu-NMe, Figure 5) was used to evaluate a selection of different methods (Monte Carlo molecular mechanics (MCMM), LMOD and mixed mode), in order to assess which would be most suitable to use for the conformational search of the peptidomimetics (see Supplemental for details). It was concluded that MCMM would be the most time effective method for providing a reasonably good representation of the conformational space for qualitative evaluation.

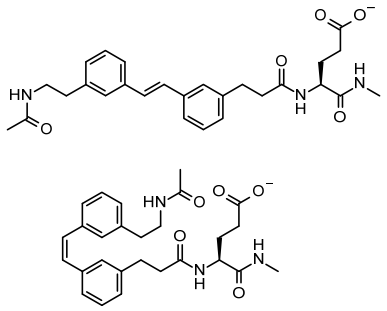

Figure 5: *E* and *Z* isomers of model compound Ac-Trigger-Glu-NMe, used for comparison of conformational search methods.

To assess whether the conformations of the peptidomimetics are markedly different in the *Z* and *E* configurations, the following approach was chosen. For molecules with a "folded" geometry (*cf. Z* configuration), a hydrogen bond between the C-terminal and N-terminal chains

is formed in most cases. Conversely, such a hydrogen bond cannot form in the *E* isomer. This intramolecular hydrogen bond was therefore used as an indicator of the overall molecular geometry. According to the computations, the probability of hydrogen bonding in the model compound (Figure 5) was 66% for the *Z* isomer, but only 8% for the *E* isomer. This should result in a more folded conformation for the *Z*-peptidomimetic compared to the corresponding *E*-peptidomimetic. Examination of all the model compound conformers supports that this is a good measurement of the actual geometry of the molecule. Therefore, this measure was also used to examine the other peptidomimetics from Table 2 by MCMM conformational searches.

To identify candidates with large geometric differences between their *Z* and *E* isomers, the results were evaluated as follows. For conformers with lowest energies, the probability of hydrogen bonding between the chains attached to the phototrigger was calculated. The conformations were then clustered, and each cluster was examined more thoroughly. This involved specifying the hydrogen bond acceptors and donors for both chains, followed by comparison of distances and angles to those atoms to identify all possibilities for hydrogen bonding. Boltzmann populations for every conformer were calculated, which then were used to estimate the total Boltzmann population for all conformers with hydrogen bonds. These populations were used as an approximate indicator of folded or extended conformation of the peptidomimetic. The procedure provides a useful measure of overall geometry for shorter peptidomimetics which essentially have two main geometries, folded or extended. However, it is less suitable for longer sequences that can adopt more complex geometries. Furthermore, since explicit solvent molecules were not included in the calculations, hydrogen bonding with the solvent is neglected, promoting intramolecular hydrogen bonds, although, since only the comparison between the two respective configurations is interesting, this error should be small.[15]

Hydrogen bonding between chains.

The probability of intramolecular hydrogen bonding is shown in Figure 6. Most of the *Z* isomers readily form hydrogen bonds, in contrast to a high variation in hydrogen bonding probability displayed by the *E* isomers (between 0 % - 95 %). Five peptidomimetics **C1** – **C5** are identified as having very different geometries between their isomers, with nearly all the conformers of the *Z* configuration forming hydrogen bonds, and almost no hydrogen bonding for *E* configuration conformers.

Qualitative inspection of the clusters indicated that the peptidomimetics with differing hydrogen bonding possibilities in *Z* and *E* configurations also have the most differing geometries. This supports the use of hydrogen bond probabilities as an indicator for the overall geometry of these peptidomimetics.

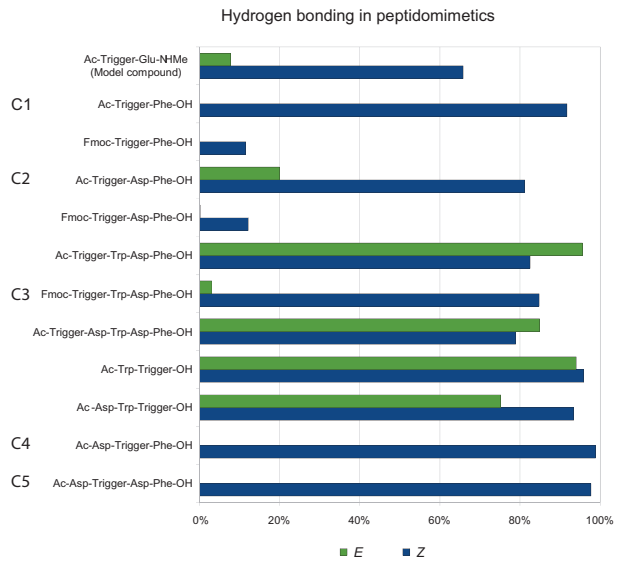

Figure 6: Percentage of hydrogen-bonded terminal chains in the peptidomimetics selected from Table 3. Candidates with the largest differences in hydrogen bond probabilities are identified as C1 – C5.

Enzyme docking

To estimate binding possibilities of the five candidates **C1** – **C5** with the RNR dimerisation site, enzyme docking with Glide was performed.[16] Glide computes different poses for each inhibitor candidate (in *Z* and *E* configurations). For all five peptidomimetics, suitable docking poses for interaction with the enzyme could be identified. An example is shown in Figure 7.

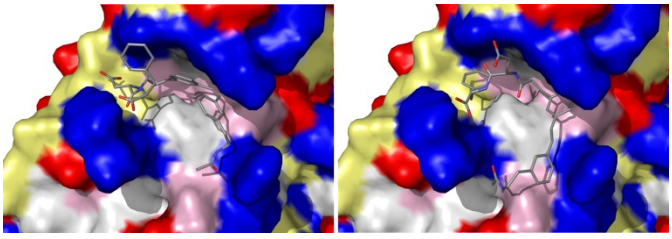

Z–**7** *E*–**7**

Figure 7: Above: The same view as in Figure 3. Residues coloured by type (blue: positive, red: negative, white: hydrophobic, pink: aromatic, yellow polar). Compound **7** docked to the dimerization site for the RNR R2 subunit. Each docking pose is shown above, *Z* to the left and *E* to the right. The peptidomimetics are shown in gray (blue nitrogens, red oxygens).

While the proposed method hardly can estimate actual affinity for the enzyme with good accuracy, it can predict whether the possibility of binding exists at all, or if some of the ligands have any flaws that makes it impossible for them to enter the binding site (*e.g.* steric hindrance). Since the five candidates **C1** – **C5** could fit into the pocket, it seems they all have potential as inhibitors of the enzyme. An interesting fact can be observed in the docking results: In all five *Z*-peptidomimetics, the stilbene residue could bind into the deep hydrophobic pocket which normally accommodates the tryptophan residue in the C-

terminal heptapeptide of R2. This interaction could not be observed with any of the *E*-peptidomimetics, since *E*-stilbene is too large to fit in this pocket. This suggests that the different isomers could have different inhibitory effect towards the enzyme.

Having established the relevancy of the computational screening method, three of the candidates for shorter druglike analogues of the C-terminal of heptapeptide R2 (Figure 8) were selected for synthesis and subsequent spectroscopic and biological evaluation. It is important to note that the results presented in Figure 6 only reflect the probability that the isomers are different in secondary structure. Therefore, the final selection was performed based on both the results from the conformational search and on rational consideration of structural characteristics. **C1** was chosen as the shortest sequence which showed a clear difference in H-bond probability between the *Z* and *E* isomers. **C2** was selected over **C3** because of shorter chain length and consistency in amino acid residues. Finally, **C5** was chosen as the longest sequence with a clear difference in secondary structure between isomers. Thus, the final set of candidates (**C1**, **C2** and **C5**, hereafter referred to as **6**, **7**, and **8**, respectively (Figure 8)) all contain the same natural amino acids and the peptide length is increased through the series.

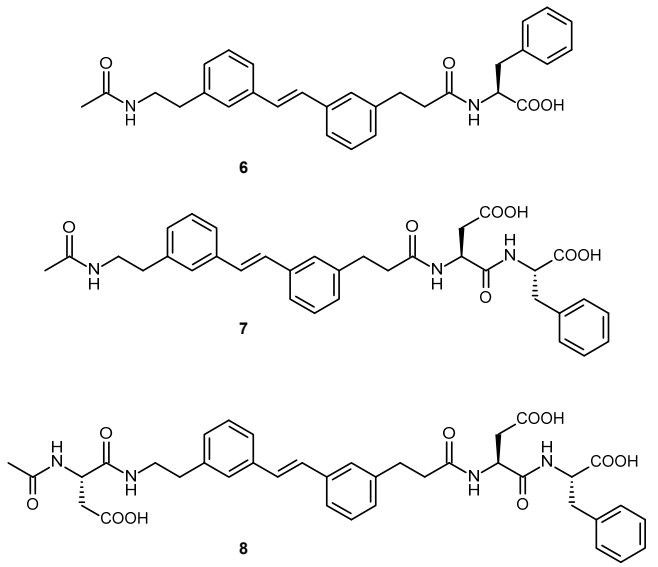

Figure 8: Phototriggerable "drug like" peptidomimetic analogues of the C-terminal heptapeptide unit of R2.

Synthesis.

Preparation of the *E* and *Z* isomers of compounds **6** – **8** followed those used for **3** – **5**.

NMR studies of peptidomimetics.

An attempt was made to spot any differences in the geometries of the peptidomimetics **6** – **8**. However, nuclear Overhauser effects were only observed between vicinal protons. The peptidomimetics are probably too short and flexible to exist in any long lived conformations on the NMR timescale. Amide proton temperature coefficients were measured to identify NH hydrogen bonds.[17] These figures (Table 4) indicate that none of the amide protons form hydrogen bonds in the *E* isomers, but that some do in the *Z* isomers. Interestingly, the NH protons that participate in hydrogen bonding are the ones that belong to the Asp-Phe peptide bond, as well as the trigger-NH in Z–**8**. These results indicate that the peptidomimetics are more flexible in the *E* form than in the *Z* form, in agreement with the computational predictions.

Table 4: Amide proton temperature coefficients of the peptidomimetics, reported as -dδ/dT in ppb/K. Figures that indicate hydrogen bonding (< 4.6 ppb/K) in bold. Solvent: DMSO-d_6.

Sequence	Residue	*Z*	*E*
Ac-Trigger-Phe-OH	Trigger	4.87	5.58
(**6**)	Phe	5.68	6.23
Ac-Trigger-Asp-Phe-OH	Trigger	5.03	5.60
(**7**)	Asp	5.48	4.84
	Phe	**2.03**	5.85
Ac-Asp-Trigger-Asp-Phe-OH	Asp1	5.29	5.38
(**8**)	Trigger	**4.37**	5.81
	Asp2	6.28	5.03
	Phe	**1.30**	5.54

Binding studies Method B

The affinity of compounds **6** – **8** as binders to *Mycobacterium tuberculosis* RNR was evaluated using the same competitive fluorescence polarization assay as in Method A. However, instead of determining DC_{50} the dissociation constant K_{D2} for the interaction between a compound and the target enzyme was determined. The evaluation method was chosen in order to allow comparison to previously reported values from a screening study of small-molecule inhibitors for the same target enzyme.[7]

This was done by first calculating the direct dissociation constant K_{D1} between the labelled heptapeptide and the enzyme, using the direct binding model ((1) in Figure 9). K_{D1} was evaluated to be 2.2 μM. With K_{D1} determined, it is possible to determine dissociation constant K_{D2} between our unlabelled compounds and the enzyme by applying the complete competitive model ((2) in Figure 10).

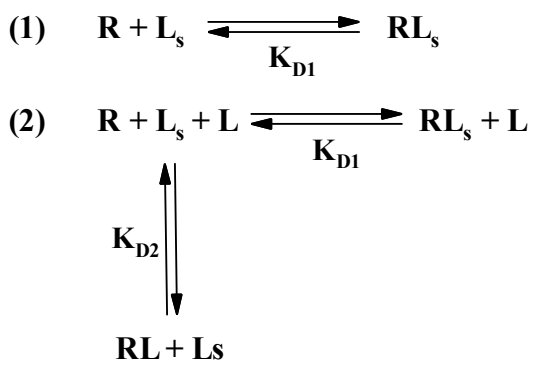

Figure 9: Direct binding model (1), and the complete competitive model (2). The following definitions are used: R, free enzyme; L, free unlabelled ligand (compounds **6** – **8**); L_s, free labelled ligand (dansylated heptapeptide); K_{D1}, dissociation constant between free enzyme and the probe; K_{D2}, dissociation constant between free enzyme and compounds **6** – **8.**

Table 5: Binding affinity phototriggerable drug like derivatives **6** – **8.**

Peptide	Inhibition K_{D2} (μM)	Relative inhibition[a]	Inhibition increase upon phototriggering[b]
Ac-**1**	8.3	1	-
Fmoc-**1**	0.7	12	-
6-*E*	23.9	0.35	57 %
6-*Z*	15.2	0.55	
7-*E*	9.9	0.83	154 %
7-*Z*	3.9	2.12	
8-*E*	8.2	1.01	55 %
8-*Z*	5.3	1.57	

Calculated with K_{D1} = 2.2 μM.
[a]Relative inhibition is presented as $K_{D2}(1)/K_{D2}(x)$. [b]$(K_{D2}(E)- K_{D2}(Z))/ K_{D2}(Z) \cdot 100$ %.

As observed with compounds **3** – **5**, the introduction of the stilbene phototrigger makes all three peptides exhibit different bonding affinities in their respective isomeric forms. Although, the relative inhibition of both *Z* and *E* forms decreased in the shorter derivatives, the dissociation constants were still lower than those of previously reported peptide inhibitors of similar length.[7] Unlike the case with the heptapeptide derivatives **3** – **5**, but in accordance with the results from the computational docking studies, it is the *Z* form that has the higher binding potency towards the target protein.

Conclusions

We have demonstrated that integrating a small phototriggerable unit into a known heptapeptide inhibitor for *Mycobacterium tuberculosis* RNR can enable modulation of its secondary structure to significantly affect its inhibitory potency. In two out of three cases, the *E* isomer was the better binder and one of these derivatives displayed a near 200 % higher affinity to the enzyme than the *Z* form. Introduction of the trigger at the N-terminal of the peptide also resulted in an increase in binding affinity. This suggests that interactions between the inhibitor and the aromatic residues at the R1 interaction site play an important role for binding, and is in accordance with previous findings.[7] A set of small phototriggerable drug like inhibitors based on truncated sequences of the known peptide inhibitor have also been designed computationally, synthesized and evaluated for binding to *Mycobacterium tuberculosis* RNR. These derivatives demonstrate the reverse binding preference, where the *Z* isomers bind better than the *E* forms. It is likely that these shorter compounds can bind to the enzyme in a less specific conformation. The fact that a clear preference for one of the isomers still can be observed could be because the *Z* isomer more resembles the bound conformation when in solution. Despite showing weaker binding affinity than the heptapeptide inhibitors, they still bind tighter than corresponding peptides without the trigger.[7] The results indicate that integration of a flexible stilbene based phototrigger into a peptide is a feasible approach for photomodulation of enzyme activity, since it has previously been shown that the catalytic activity of RNR can be inhibited by compound Ac-**1**.[7a] It is also evident that the aromatic groups of the trigger have a significant impact on the affinity. Furthermore, this paper shows that interstrand hydrogen bond probability can be a useful guideline for predicting conformational preference in small inhibitor molecules.

Experimental

NMR spectra were recorded on Bruker AVANCE III (^{1}H 600 MHz, ^{13}C 150MHz), Varian Unity Inova (^{1}H 499.9 MHz, ^{13}C 125.7 MHz), Varian Unity (^{1}H 399.5 MHz, ^{13}C 100.6 MHz) or Varian Mercury Plus (^{1}H 300.0 MHz, ^{13}C 75.5 MHz) spectrometers. Chemical shifts are referenced indirectly to tetramethylsilane *via* the residual solvent signals (^{1}H: $CHCl_3$ at 7.26, HDO at 4.79, DMSO-d_5 at 2.49. ^{13}C: $CDCl_3$ at 77.0). Signal assignments were derived from ^{1}H, ^{13}C, COSY,[18] P.E.COSY,[19] TOCSY,[20] gHSQC,[21] gHMBC,[22] NOESY[23] and ROESY[24] spectra. NMR spectra of peptidomimetics were recorded for DMSO-d_6 solutions, both on pure *E* peptidomimetics and on a mixture of *Z* and *E* peptidomimetics. Amide proton temperature coefficients $(\delta_{T,high}-\delta_{T,low})/(T_{high}-T_{low})$ were determined from series of ^{1}H NMR spectra at 25, 50, 70 and 90 °C. Temperature coefficients are obtained as negative numbers, but are reported as positive values, in accordance with the accepted literature procedure.[17] Amino acid analyses were performed at the Department of Chemistry, Biomedical Centre, Uppsala, Sweden, on 24 h hydrolyzates with an LKB 4151 Alpha Plus analyzer, using ninhydrin detection. Compounds 2 and 10 through 19 have been reported previously. See Supplementary for experimental details. Photochemical reactions were performed on DMSO-d_6 solutions under N_2 gas flow using an Oriel 1000 W Xe ARC light source and a 300 nm Oriel UV filter for 1.5–5.5 h, with a conversion to the *Z* form of 70-80 %. Quantum yields were determined by using (*E*)-Stilbene (Φ = 0.45) as an actinometer.[25]

Conformational analyses and docking studies

All structures were built with Maestro 9.0.211 and all calculations were performed on these structures from the Maestro interface. Local energy minimisation of all structures was performed with MacroModel 9.7[26] in Maestro with the OPLS 2005 force field with water as solvent using a water continuum solvation model. The minimisation method was PRCG with at most 10 000 steps. Conformational searches were performed with MacroModel on structures minimised to local minima as described above. The MCMM method[27] with 2000 steps per rotatable bond was used for searching the peptidomimetics. Minimisation conditions were the same as for local energy minimisation. The number of torsion rotations in each step was chosen randomly between 1 and N-1 (N is the number of rotatable bonds). The energy window for retaining structures was 21.0 kJ/mol and the criterion for considering structures to be similar was a maximum atom deviation of 0.5 Å. All heavy atoms were used as comparison atoms. Parameters for conformational searches in the method evaluation are described in the supplementary material. Clustering of conformers was performed with XCluster on conformers superpositioned on the four central carbon atoms in the stilbene trigger. In some cases redundant conformer elimination was performed before clustering to reduce the number of input structures to less than 2 000. Atoms used for comparison by XCluster were chosen as all heavy atoms in the chains connected to the trigger, except for atoms equivalent to one another (*e.g.* oxygens in COO^- groups). Structures were compared "in place", without further superpositioning. The clustering level (*i.e.* how many clusters to form) was chosen to obtain a small number of clusters with reasonably similar structures in every group.[28] Docking studies were performed using Glide 5.5.[16] The protein was prepared using the Protein preparation Wizard in Maestro using default settings.

Peptide synthesis

Peptides **3** – **8** were prepared manually or with automated peptide synthesizer (Pioneer, Applied Biosystems) by standard Fmoc-chemistry (9-fluorenylmethoxycarbonyl) on 0.1-0.2 mmol scale. The solid phase used was 2-chlorotrityl chloride resin with 0.2 mmol g^{-1} or 0.50 mmol g^{-1} loading. The Fmoc amino acids were coupled in four-fold excess with HBTU (0.8 M in DMF) and DIPEA (1 M in DMF) as activators. The Fmoc protecting group was deprotected by 20 % piperidine in DMF (v/v). Standard coupling times for the amino acids was 90 min, including capping with acetic anhydride after each step. The Fmoc protected stilbene derivative and the possible amino acids thereafter, were introduced manually to minimize excess using PyBop as activating agent (0.6M), a threefold excess of amino acid and allowing a coupling time of 120 min. Cleavage of the peptide was carried out in a mixture containing TFA/triethylsilane/H_2O (95:2.5:2.5 v/v) for 3 × 1 h. The TFA was concentrated and the peptides were lyophilized prior to purification.

Purification of peptides **3** – **5** was performed by preparative HPLC on a Gilson system (Gilson 231 XL Injector, 118 UV/VIS detector, Gilson syringe pump, Gilson 333 and 334 pumps and Gilson FC204) connected to a Grace Vydac C18 (22 × 250 mm, 5 µm) with a gradient of MeCN in 0.1 % aq TFA (20-60%, 60 min) Purification of 6-8 was achieved on a preparative HPLC system with an ACE5 C18 column (150 × 21.2 mm) using a gradient eluent of MeOH in water, with addition of 0.1 % formic acid, at a flow rate of 15 ml/min. The method of detection was UV absorbance at 215 and 300 nm. The collected fractions were analysed with LC-MS using a Chromolith Performance RP-18e column (4.6 × 100 mm), or by analytical HPLC using a Chromolith Performance RP-18e column (4.6 × 100 mm). The ESI-MS data were obtained with a Finnigan ThermoQuest AQA mass spectrometer (ESI 30 eV, probe temperature 100°C) equipped with a Gilson 322-H2 gradient pump system. A water-MeCN-formic acid (0.05 %) mobile phase was used with a gradient of 20 % to 100 % MeCN during 3-5 minutes.

***E*-H_2N-Trigger-Glu-Asp-Asp-Asp-Trp-Asp-Phe-OH** (**3**) (69 mg, 57 µmol, 28%). MS (ESI, 30eV) m/z (%): 611.0 (100, $[M+2H]^{2+}$), 1220.6 (30, $[M+H]^+$). Amino acid analysis: 4.19 Asp, 1.09 Glu, 1.07 Phe, 0.66 Trp.

(*Z*-isomer, 4.7 mg of E-isomer was irradiated for 120 min to a 43:57 *Z*:*E* mixture Φ= 0.20).

***E*-Ac-Trigger-Glu-Asp-Asp-Asp-Trp-Asp-Phe-OH** (**4**) (61 mg, 48 µmol, 24%). MS (ESI, 30eV) m/z (%): 631. (100, $[M+2H]^{2+}$), 1260.8 (10, $[M+H]^+$). Amino acid analysis: 4.04 Asp, 1.17 Glu, 1.11 Phe, 0.67 Trp.

(*Z*-isomer, 4.2 mg of E-isomer was irradiated for 120 min to a 44:66 *Z*:*E* mixture Φ= 0.18).

***E*-Ac-Trp-Trigger-Glu-Asp-Asp-Asp-Trp-Asp-Phe-OH** (**5**) (57 mg, 39 µmol, 20%). MS (ESI, 30eV) m/z (%): 724.2 (40, $[M+2H]^{2+}$), 1447.7 (100, $[M+H]^+$). Amino acid analysis: 4.30 Asp, 1.06 Glu, 1.03 Phe, 1.61 Trp.

(*Z*-isomer, 4.2 mg of E-isomer was irradiated for 120 min to a 44:66 *Z*:*E* mixture Φ= 0.16).

***E*-Ac-Trigger-Phe-OH** (**6**) (9.8 mg, 19 µmol, 19%). ^{1}H NMR: (500 MHz, DMSO-d_6) δ = 1.80 (s, 3H, CH_3), 2.41 (t, J = 7.5 Hz, 2H, CH_2), 2.72 (m, 3H, CH_2, CH_2), 2.85 (dd, J = 14.0, 9.3 Hz, 1H, Phe-H_β), 3.03 (dd, J = 14.0, 5.2 Hz, 1H, Phe-H_β), 3.29 (dt, J = 7.5, 7.5 Hz, 2H, CH_2), 4.43 (ddd, J = 9.3, 8.2, 5.2 Hz, 1H, Phe-H_α), 7.04 (d, J = 7.5 Hz, 1H, ArH), 7.11 (d, J = 7.5 Hz, 1H, ArH), 7.18 (m, 3H, ArH), 7.21 (2 AB-d, , 2H, HC=CH), 7.25 (m, 3H, ArH), 7.29 (t, J = 7.5 Hz, 1H, ArH), 7.43 (m, 4H, ArH), 7.94 (t, J = 7.5 Hz, 1H, Trigger-NH), 8.19 (d, J = 8.2 Hz, 1H, Phe-NH).
Z-isomer: 5.2 mg of *E*-isomer was irradiated for 330 min to afford a 70:30 Z:E mixture, Φ= 0.25; δ = 1.76 (s, 3H, CH_3),

2.27 (dd, J = 8.8, 6.4 Hz, 2H, CH_2), 2.57 (m, 3H, CH_2, CH_2), 2.83 (m, 1H, Phe-H_β), 3.03 (m, 1H, Phe-H_β), 3.15 (ddd, J = 8.0, 7.2, 5.5 Hz, 2H, CH_2), 4.29 (m, 1H, Phe-H_α), 6.57 (2 AB-d, , 2H, HC=CH), 7.05 (m, 12H, ArH), 7.44 (dm, J = 7.6 Hz, 1H, ArH), 7.83 (br s, 1H, Phe-NH), 7.92 (t, J = 5.5 Hz, 1H, Trigger-NH).
MS (ESI, 30 eV) m/z (%): 485.5 (100, $[M+H]^+$).

***E*-Ac-Trigger-Asp-Phe-OH (7)** (4,1 mg, 6.83 µmol, 7%). ^{1}H NMR: (500 MHz, DMSO-d_6) δ =1.80 (s, 3H, CH_3), 2.42 (m, 3H, H_β-Asp, CH_2), 2.64 (dd, J = 16.3, 5.9 Hz, 1H, H_β-Asp), 2.72 (t, J = 7.5 Hz, 2H, CH_2), 2.80 (t, J = 7.5 Hz, 2H, CH_2), 2.91 (dd, J = 13.7, 7.6 Hz, 1H, H_β-Phe), 3.02 (dd, J = 13.7, 5.3 Hz, 1H, H_β-Phe), 3.30 (dt, J = 7.5, 5.6 Hz, 2H, CH_2), 4.40 (ddd, J = 8.3, 7.6, 5.3 Hz, 1H, H_α-Phe), 7.11 (d, J = 7.7 Hz, 2H, ArH), 7.21 (m, 7H, ArH), 7.22 (2 AB-d, 2H, HC=CH), 7.40 (m, 4H, ArH), 7.63 (ddd, J = 8.3, 7.4, 5.9 Hz, 1H, H_α-Asp), 7.92 (d, J = 8.3 Hz, 1H, NH-Phe), 7.94 (t, J = 5.6 Hz, 1H, NH-Trigger), 8.16 (d, J = 8.3 Hz, 1H, NH-Asp).

Z-isomer: 2.5 mg of E-isomer was irradiated for 240 min to afford a 72:28 *Z*:*E* mixture, Φ= 0.20; δ = 1.76 (s, 3H, CH_3), 2.31 (m, 3H, H_β-Asp, CH_2), 2.59 (t, J = 7.4 Hz, 1H, CH_2), 2.68 (m, 3H, Hβ-Asp, CH_2), 2.92 (m, 1H, H_β-Phe), 2.99 (m, 1H, H_β-Phe), 3.19 (dt, J = 13.0, 6.4 Hz, 2H, CH_2), 4.19 (m, 1H, H_α-Phe), 4.56 (ddd, J = 7.4, 7.4, 7.4 Hz, 1H, H_α-Asp), 6.58 (2 AB-d, 2H, HC=CH), 7.17 (m, 12H, ArH), 7.45 (m, 1H, ArH), 7.69 (br s, 1H, NH-Phe), 7.97 (t, J = 6.4 Hz, 1H, NH-Trigger), 8.01 (br s, 1H, NH-Asp).
MS (ESI, 30 eV) m/z (%): 600.5 (100, $[M+H]^+$).

***E*-Ac-Asp-Trigger-Asp-Phe-OH (8)** (4.3 mg, 6.02 µmol 7%). ^{1}H NMR: (500 MHz, DMSO-d6) δ = 1.82 (s, 3H, CH_3), 2.41 (m, 4H, H_β-Asp1, H_β-Asp2, CH_2), 2.59 (dd, J = 16.0, 5.7 Hz, 1H, H_β-Asp1), 2.63 (dd, J = 16.0, 5.1 Hz, 1H, H_β-Asp2), 2.71 (t, J = 7.2 Hz, 2H, CH_2), 2.79 (t, J = 7.9 Hz, 2H, CH_2), 2.91 (dd, J = 14.0, 8.0 Hz, 1H, H_β-Phe), 3.02 (dd, J = 14.0, 5.1 Hz, 1H, H_β-Phe), 3.28 (dt, J = 7.2, 5.6 Hz, 2H, CH_2), 4.36 (ddd, J = 8.0, 7.4, 5.5 Hz, 1H, H_α-Phe), 4.51 (ddd, J = 8.0, 7.4, 5.7 Hz, 1H, H_α-Asp1), 4.60 (ddd, J = 8.0, 7.4, 5.1 Hz, 1H, H_α-Asp2), 7.10 (d, J = 7.3 Hz, 2H, ArH), 7.20 (m, 7H, ArH), 7.21 (2 AB-d, 2H, HC=CH), , 7.42 (m, 4H, ArH), 7.87 (d, J = 7.4 Hz, 1H, NH-Phe), 7.92 (t, J = 5.6 Hz, 1H, NH-Trigger), 8.11 (d, J = 8.0 Hz, 1H, NH-Asp1), 8.17 (d, J = 8.0 Hz, 1H, NH-Asp2).

Z-isomer: 2.3 mg of E-isomer was irradiated for 330 min to afford a 81:28 *Z*:*E* mixture, Φ=0.18; δ = 1.81 (s, 3H, CH_3), 2.43 (m, 4H, H_β-Asp1, H_β-Asp2, CH_2), 2.54 (m, 4H, H_β-Asp1, H_β-Asp2, CH_2), 2.63 (m, 2H, CH_2), 2.92 (m, 1H, H_β-Phe), 3.01 (m, 1H, H_β-Phe), 3.12 (m, 2H, CH_2), 4.21 (m, 1H, H_α-Phe), 4.52 (m, 2H, H_α-Asp1, H_α-Asp2), 6.58 (2 AB-d, 2H, HC=CH), 7.15 (m, 12H, ArH), 7.42 (m, 1H, ArH), 7.67 (br s, 1H, NH-Phe), 7.96 (br s, 1H, NH-Trigger), 8.13 (m, 2H, NH-Asp1, NH-Asp2).
MS (ESI, 30 eV) m/z (%): 715.4 (100, $[M+H]^+$).

Binding assay (**3** – **8**)

The synthesis of the fluorescent probe was carried out on solid phase using Fmoc/t-Bu protection scheme. The fluorescent probe high throughput screening (FT-HTS) of **3** – **8** was performed with a 2102 EnVision multilabel plate reader (PerkinElmer). Corning Costar 384-well black plates were used for the assay. To each well was added 200 nM R1, 50 nM dansylated heptapeptide, inhibitors (in the concentration range from 10 to 100 µM) and the reaction buffer (0.05 % Triton x-100, 10 mM NDSB195 and 5 mM Hepes pH 7) to a final reaction volume of 50 µl. The mixture was incubated for 2 min at room temperature. Exitation was done with polarized light with a wavelength of 333 nm at room temperature, and detection of the emission was done at 518 nm. Fluorescence polarization was calculated according to the function $FP = (I^{=} - I^{\perp})/(I^{=} + I^{\perp})$ where $I^{=}$ and $I^{\perp}$ is the intensity of the emitted parallel and vertical beam.

Acknowledgements

Financial support by the Swedish Foundation for Strategic Research (SSF) and by the Swedish Research Council (VR) are gratefully acknowledged. We also thank Per I. Arvidsson (UU) and Gert Kruger (UKZN) for supporting an exchange visit at the University of KwaZulu-Natal through their bi-lateral Sweden-South Africa Research Link program. Gert Kruger is also acknowledged for his hospitality during the stay at UKZN. Torsten Unge (UU) is acknowledged for providing access to the binding assay.

Notes and references

Electronic Supplementary Information (ESI) available: [experimental details for syntheses and computations, NMR spectra of compounds **3** – **8**]. See DOI: 10.1039/b000000x/

1. (a) G. Mayer, A. Heckel, *Angew. Chem. Int. Ed.*, 2006, **45**, 2900; (b) C. Renner, L. Moroder, *ChemBioChem.*, 2006, **7**, 868; (b) O. Khakshoor, J. S. Nowick, *Curr. Opin. Chem. Biol.*, 2008, **12**, 722; (c) A. Beharry, G. A. Wolley, *Chem. Soc. Rev.*, 2011, **40**, 4422; (d) C. Brieke, F. Rohrbach, A. Gottschalk, G. Mayer, A. Heckel, *Angew. Chem. Int. Ed.*, 2012, **51**, 8446; (e) W. Szymański, J. M. Beierle, H. A. V. Kistemaker, W. A. Velema, B. L. Feringa, *Chem. Rev.*, 2013, **113**, 6114; (f) W. A. Velema, W. Szymanski, B. L. Feringa, *J. Am. Chem. Soc*., 2014, **136**, 2178.
2. (a) M. Andersen, M. C. Wahl, A. C. Stiel, F. Gräter, L. V. Schäfer, S. Trowitzsch, G. Weber, C. Eggeling, H. Grubmüller, S. W. Hell, S. Jakobs, *Proc. Natl. Acad. Sci. USA*, 2005, **102**, 13070. (b) L. V. Schäfer, G. Groenhof, A. R. Klingen, G. M. Ullmann, M. Boggio-Pasqua, M. A. Robb, H. Grubmüller, *Angew. Chem. Int. Ed.*, 2007, **119**, 536; (c) R. Ando, H. Hama M. Yamamoto-Hino, H. Mizunou, A. Miyawaki, *Proc. Natl. Acad. Sci. USA*, 2002, **99**, 12651; (d) O. V. Stepanenko, O. V. Stepanenko, D. M. Shcherbakova, I. M. Kuznetsova, K. K. Turoverov, V. V. Verkhusha, *Biotechniques*, 2011, **51**, 313.

3. (a) C. Dugave, L. Demange, *Chem. Rev.* 2003, **103**, 2475; (b) G. A. Woolley, *Acc. Chem. Res.*, 2005, **38**, 486; (c) J. A. Ihalainen, J. Bredenbeck, R. Pfister, J. Helbing, L. Chi, I. H. M. van Stokkum, G. A. Woolley, P. Hamm, *Proc. Natl. Acad. Sci. USA*, 2007, 104, 5383; (d) P. Hamm, J. Helbing, J. Bredenbeck, *Ann. Rev. Phys. Chem.*, 2008, **59**, 291; (e) K. Rück-Braun, S. Kempa, B. Priewisch, A. Richter, S. Seedorff, L. Wallach, *SYNTHESIS*, 2009, 4256; (f) A. M. Ali, G. A. Woolley, *Organic & Biomol. Chem.*, 2013, **11**, 5325; (g) S. Samanta, A. Babalhavaeji, M.-X. Dong, G. A. Woolley, *Angew. Chem. Int. Ed.*, 2013, **52**, 14127; (h) S. Samanta, T. M. McCormick, S. K. Schmidt, D. S. Seferos, G. A. Woolley, *Chem. Commun.,* 2013, **49**, 10314.
4. (a) M. Erdélyi, A. Karlén, A. Gogoll, *Chem. Eur. J.*, 2006, **12**, 403; (b) M. Erdélyi, M. Varedian, C. Sköld, I. B. Niklasson, J. Nurbo, Å. Persson, J. Bergquist, A. Gogoll, *Organic & Biomol. Chem.*, 2008, **6**, 4356; (c) N. J. V. Lindgren, M. Varedian, A. Gogoll, *Chem. Eur. J.*, 2009, **15**, 501; (d) M. Varedian, M. Erdélyi, Å. Persson, A. Gogoll, *J. Peptide Sci.*, 2009, **15**, 107.
5. P. Reichard, *Science*, 1993, **260**, 1773.
6. (a) S. S. Dawes, D. F. Warner, L. Tsenova, J. Timm, J. D. McKinney, G. Kaplan, H. Rubin, V. Mizrahi, *Infect. Immun.*, 2003, **71**, 6124; (b) M. B. Mowa, D. F. Warner, G. Kaplan, B. D. Kana, V. J. Mizrahi, *Bacteriol*., 2009, **191**, 985; (c) F. Yang, C. Curran, L.-S. Li, D. Avarbock, J. D. Graf, M.-M. Chua, G. Lu, J. Salem, H. J Rubin, *Bacteriol*., 1997, **179**, 6408; (d) J. Nurbo, A. K. Roos, D. Muthas, E. Wahlstrom, D. J. Ericsson, T. Lundstedt, T. Unge, A. Karlen, *J. Pept. Sci.*, 2007, **13**, 822; (e) B. Zhou, L. Su, S. Hu, W. Hu, M. L. R. Yip, J. Wu, S. Gaur, D. L. Smith, Y.-C. Yuan, T. W. Synold, D. Horne, Y. Yen, *Cancer Res.*, 2013, **73**, 6484; (f) S. Bhave, H. Elford, M. A. McVoy, *Antiviral Res.*, 2013, **100**, 151; (g) F. Tholander, B.-M. Sjöberg, *PNAS*, 2012, **109**, 9798.
7. (a) J. Nurbo, A. K. Roos, D. Muthas, E. Wahlstrom, D. J. Ericsson, T. Lundstedt, T. Unge, A. Karlen, *J. Pept. Sci.*, 2007, **13**, 822; (b) Y. Gao, S. Liehr, B. S. Cooperman, *Bioorg. Med. Chem. Lett.*, 2002, **12**, 513; (c) M. J. Fuertes, J. Kaur, P. Deb, B. S. Cooperman, A. B. Smith, *Bioorg. Med. Chem. Lett.*, 2005, **15**, 5146; (d) A. B. Smith, S. Sasho, B. A. Barwis, P. Sprengeler, J. Barbosa, R. Hirschmann, B. S. Cooperman, *Bioorg. Med. Chem. Lett.*, 1998, **8**, 3133; (e) E. K. Dziadulewicz, M. C. Brown, A. R. Dunstan, W. Lee, N. B. Said, P. J. Garratt, *Bioorg. Med. Chem. Lett.*, 1999, **9**, 463; (f) D. J. Lauffer, M. D. Mullican, *Bioorg. Med. Chem. Lett.*, 2002, **12**, 1225; (g) J. Y. Lee, I. Im, T. R. Webb, D. McGrath, M. R. Song, Y. C. Kim, *Bioorg. Chem.*, 2009, **37**, 90; (h) W. C. Ripka, G. V. Delucca, A. C. Bach, R. S. Pottorf, J. M. Blaney, *Tetrahedron*, 1993, **49**, 3609; (i) D. J. Ericsson, J. Nurbo, D. Muthas, K. Hertzberg, G. Lindeberg, A. Karlén, T. Unge, *J. Pept. Sci.*, 2010, **16**, 159; (j) J. Nurbo, D. J. Ericsson, U. Rosenström, D. Muthas, A. M. Jansson, G. Lindeberg, T. Unge, A. Karlén, *Biorg. Med. Chem.*, 2013, **21**, 1992.
8. (a) J. Kuil, L. T.M. van Wandelen, N. J. de Mol, R. M. J. Liskamp, *J. Pept. Sci.* 2009, **15**, 685; (b) D. Kraskouskaya, E. Duodu, C. C. Arpinw, P. T. Gunning, *Chem. Soc. Rev.*, 2013, **42**, 3337.
9. H. Lebel, O. Leogane, *Org. Lett.*, 2005, **7**, 4107.
10. G. M. Sammis, E. N. Jacobsen, *J. Am. Chem. Soc.*, 2003, **125**, 4442.
11. J. H. Zhang, T. D. Chung, K. R. Oldenburg, *J. Biomol. Screen.*, 1999, **4**, 67.
12. J. Vagner, H. Qu, V. J. Hruby, *Curr. Opin. Chem. Biol.*, 2008, **12**, 292.
13. P. K. Gadakar, S. Phukan, P. Dattatreya, V. N. Balaji, *J. Chem. Inf. Model.*, 2007, **47**, 1446.
14. M. Uppsten, M. Färnegårdh, V. Domkin, U. Uhlin, *J. Mol. Biol.*, 2006, **359**, 365.
15. W. C. Still, A. Tempczyk, R. C. Harvey, T. Hendrickson, *J. Am. Chem. Soc.* 1990, **112**, 6127
16. R. A. Friesner, J. L. Banks, R. B. Murphy, T. A. Halgren, J. J. Klicic, D. T. Mainz, M. P. Repasky, E. H. Knoll, M. Shelley, J. K. Perry, D. E. Shaw, P. Francis, P. S. Shenkin *J. Med. Chem.*, 2004, **47**, 1739.
17. (a) H. Kessler, *Angew. Chem.,* 1982, 94, 509; (b) T. Cierpicki, J. Otlewski, *J. Biomol. NMR*, 2001, **21**, 249; (c) M. Erdélyi, V. Langer, A. Karlén, A. Gogoll, *New J. Chem.,* 2002, **26**, 834.
18. (a) Wokaun, R. R. Ernst, *Chem. Phys. Lett.*, 1977, **52**, 407; (b) A. J. Shaka, R. Freeman, *J. Magn. Reson.*, 1983, **51**, 169.
19. L. Mueller, *J. Magn. Reson.*, 1987, **72**, 191.
20. L. Braunschweiler, R. R. Ernst, *J. Magn. Reson.*, 1983, **53**, 521.
21. L. Davis, J. Keeler, E. D. Laue, D. Moskau, *J. Magn. Reson.*, 1992, **98**, 207.
22. R. E. Hurd, B. K. John, *J. Magn. Reson.*, 1991, **91**, 648.
23. (a) Kumar, R. R. Ernst and K. Wüthrich, *Biochem. Biophys. Res. Commun.*, 1980, **95**, 1; (b) G. Bodenhausen, H. Kogler and R. R. Ernst, *J. Magn. Reson.*, 1984, **58**, 370.
24. Bax, D. G. Davis, *J. Magn. Reson.*, 1985, **63**, 207.
25. T.-I. Ho; T.-M. Su; T.-C. Hwang, *J. Photochem. Photobiol. A: Chemistry*, 1983, **41**, 293.
26. F. Mohamadi, N. G. J. Richards,W. C. Guida, R. Liskamp, M. Lipton, C. Caufield, G. Chang, T. Hendrickson and W. C. Still, *J. Comput. Chem.*, 1990, **11**, 440.
27. G. Chang, W. C. Guida, C. Still, *J. Am. Chem. Soc.*, 1989, **111**, 4379.
28. P. S. Shenkin, D. Q. McDonald, *J. Comput. Chem.*, 1994, **15**, 899.

Peptidomimetic inhibitors with photomodulable affinity for the R1 - R2 subunit association site of a bacterial ribonucleotide reductase were designed based on the R2-subunit C-terminal.